



RESEARCH ARTICLE

Temporin G, an amphibian antimicrobial peptide against influenza and parainfluenza respiratory viruses: Insights into biological activity and mechanism of action

M. De Angelis¹ | B. Casciaro² | A. Genovese¹ | D. Brancaccio³ |
 M. E. Marcocci¹ | E. Novellino³ | A. Carotenuto³ | A. T. Palamara¹ |
 M. L. Mangoni⁴  | L. Nencioni¹ 

¹Department of Public Health and Infectious Diseases, Laboratory Affiliated to Pasteur Italia-Fondazione Cenci Bolognetti, Sapienza University of Rome, Rome, Italy

²Center For Life Nano Science@Sapienza, Istituto Italiano di Tecnologia, Rome, Italy

³Department of Pharmacy, University of Naples "Federico II", Naples, Italy

⁴Department of Biochemical Sciences, Laboratory Affiliated to Pasteur Italia-Fondazione Cenci Bolognetti, Sapienza University of Rome, Rome, Italy

Correspondence

L. Nencioni, Department of Public Health and Infectious Diseases, Laboratory Affiliated to Pasteur Italia-Fondazione Cenci Bolognetti, Sapienza University of Rome, Piazzale Aldo Moro, 5, Rome 00185, Italy.
 Email: lucia.nencioni@uniroma1.it

M. L. Mangoni, Department of Biochemical Sciences, Laboratory Affiliated to Pasteur Italia-Fondazione Cenci Bolognetti, Sapienza University of Rome, Piazzale Aldo Moro, 5, Rome, Italy.
 Email: marialuisa.mangoni@uniroma1.it

Funding information

Italian Ministry of Instruction, Universities and Research, Grant/Award Number: MIUR PRIN 2017 2017BMK8JR006 and MIUR PONARS 01_00597_OR4; Fondazione Cenci Bolognetti Istituto Pasteur Italia; Pasteur-Italia Fondazione Cenci Bolognetti "Anna Tramontano 2018"; Sapienza University, Grant/Award Number: RM11816436113D8A

Abstract

Treatment of respiratory viral infections remains a global health concern, mainly due to the inefficacy of available drugs. Therefore, the discovery of novel antiviral compounds is needed; in this context, antimicrobial peptides (AMPs) like temporins hold great promise. Here, we discovered that the harmless temporin G (TG) significantly inhibited the early life-cycle phases of influenza virus. The *in vitro* hemagglutinating test revealed the existence of TG interaction with the viral hemagglutinin (HA) protein. Furthermore, the hemolysis inhibition assay and the molecular docking studies confirmed a TG/HA complex formation at the level of the conserved hydrophobic stem groove of HA. Remarkably, these findings highlight the ability of TG to block the conformational rearrangements of HA2 subunit, which are essential for the viral envelope fusion with intracellular endocytic vesicles, thereby neutralizing the virus entry into the host cell. In comparison, in the case of parainfluenza virus, which penetrates host cells upon a membrane-fusion process, addition of TG to infected cells provoked ~1.2 log reduction of viral titer released in the supernatant. Nevertheless, at the same condition, an immunofluorescent assay showed that the expression of viral hemagglutinin/neuraminidase protein was not significantly reduced. This suggested a peptide-mediated block of some late steps of viral replication and therefore the impairment of the extracellular release of viral particles. Overall, our results are the first

Abbreviations: CC₅₀, 50% cytotoxic concentration; DMEM, Dulbecco's modified Eagle medium; DPC, dodecylphosphocholine; FBS, fetal bovine serum; MTT, 3-(4,5-dimethylthiazol-2-yl)-2,5-diphenyltetrazolium bromide; HA, hemagglutinin; HAU, hemagglutinating unit; HN, parainfluenza hemagglutinin-neuraminidase; HPLC, high-performance liquid chromatography; ICW, in-cell western; NA, neuraminidase; NP, nucleoprotein; PBS, phosphate buffered saline; RBCs, red blood cells; RFI, relative fluorescence intensity; SDS, sodium dodecyl sulfate; TCID₅₀, tissue culture infectious dose 50%; T-TBS, Tween 20+ Tris-buffered saline.

M. L. Mangoni and L. Nencioni equally contributed to the work.

demonstration of the ability of an AMP to interfere with the replication of respiratory viruses with a different mechanism of cell entry and will open a new avenue for the development of novel therapeutic approaches against a large variety of respiratory viruses, including the recent SARS-CoV2.

KEYWORDS

antimicrobial peptides, antiviral agents, influenza, parainfluenza, viral infection

1 | INTRODUCTION

Influenza viruses are among the most common infectious human respiratory pathogens associated with significant morbidity and mortality, especially from hospital settings, accounting for about 290 000–650 000 fatal cases per year.¹ They are responsible for annual epidemics disease (known as the flu season), which takes place during autumn and winter in temperate climates, and occasionally for pandemic events. Flu usually arises with non-specific symptomatology, described by cold, fever, intense headache, cough, and inflammation of the respiratory tract.² Influenza virus type A particles have a double lipid layer, namely envelope, where two membrane glycoproteins, ie, hemagglutinin (HA) and neuraminidase (NA) as well as the matrix M2 protein are inserted.^{3,4} While HA, in the form of trimer, and NA in the form of tetramer project toward the outside of the virion for about 10–14 nm forming the so-called *spikes*, M2 protein is an ion channel that favors the viral uncoating.^{5,6} The genome consists of a negative sense, single-stranded, segmented RNA. Each viral RNA (vRNA) segment is associated with the nucleoprotein (NP) and the heterotrimeric complex of RNA-dependent RNA-polymerase, forming the helical ribonucleoprotein capsids (vRNPs).^{5,7} The life-cycle of influenza virus encompasses six major steps: (i) the entry of viral particles into the host cell by HA-sialic acid-mediated endocytosis; (ii) fusion of the viral envelope with the intracellular endosome allowing viral uncoating; (iii) nuclear import of vRNPs; (iv) transcription and replication of the viral genome; (v) export of the vRNPs from the nucleus; (vi) post-translational modification followed by packaging, budding and release of viral particles from the host cell membrane.⁸ Influenza virus infections can be controlled through vaccination and/or antiviral drugs. Nevertheless, despite vaccination reduces the number of sick human subjects as well as the spread of the virus mainly among people most exposed to the risk of post-flu complications, the vaccine product must be constantly updated due to the genetic instability of the virus.⁹ In contrast, antiviral agents represent a useful and efficacious tool for treating flu in the absence of an appropriate vaccine (particularly in the case of a pandemic). Currently, three families of antiviral compounds have been developed against

influenza A virus.¹⁰ The first one blocks the ion-channel activity of the viral M2 protein, which is mainly required for virus uncoating; the second family includes inhibitors of the viral NA, which allows the release of viral particles from infected cells; more recently a new family of compounds has been developed against the polymerase complex and two of them, ie, baloxavir marboxil and favipiravir, have being licensed in Japan and United States.¹⁰ However, the huge circulation of different influenza viruses and the emergence of drug-resistant strains stand for a global serious challenge to human health, making the identification of new antiviral compounds a pressing need.¹¹

The evolutionarily conserved naturally occurring antimicrobial peptides (AMPs), also named host defense peptides are key factors of the innate immunity in almost all living organisms and have opened the door to the current field of drug discovery.^{12,13} Yet, only a few reports on the antiviral activity of AMPs are available so far.¹⁴ The granular glands of amphibian skin produce an extraordinarily large variety of AMP families.^{15,16} Among them, the frog skin temporins count more than 1000 members.¹⁵ They are very short molecules (generally containing 10–13 amino acids) with a net charge ranging from +1 to +3 and with the ability to adopt an amphipathic alpha-helical conformation when in contact with biological membranes.¹⁷ Their principal mechanism of antibacterial activity relies on the perturbation of the target microbial cell membrane.^{18,19} This makes AMPs less prone to induce resistance compared to conventional drug therapies. In fact, acquisition of resistance to AMPs would imply a consistent change in the microbial phospholipid bilayer; a process not compatible with the survival of microbes. Noteworthy, besides displaying a strong bactericidal and antiprotozoal activity,^{19,20} some temporin isoforms have already shown the capability to inhibit the replication of human enveloped viruses, such as herpes simplex virus 1 (HSV-1).²¹ Recent studies have highlighted a virucidal effect of temporin B (TB), likely due to the peptide-induced physical disruption of the HSV-1 envelope, as confirmed by electron microscopy.²¹ Here we screened temporins A, B, and G (TA, TB, TG) from *Rana temporaria* for their efficacy against human influenza virus type A. By using a concerted multidisciplinary approach based on molecular biology, biochemical and computational studies, we identified TG as a powerful agent able to inhibit the virus entry into the cell. In parallel, the ability of the most

promising TG to hinder the release of parainfluenza virus particles from infected cells was also discovered. Importantly, this is the first demonstration of an isoform of temporins, and generally of AMPs, to differently hamper the replication of respiratory viruses. Overall, besides getting insight into the plausible mechanism underlying the activity of temporins against respiratory viruses, this work should assist the design and development of novel therapeutic agents for the treatment of flu.

2 | MATERIALS AND METHODS

2.1 | Reagents

Dulbecco's modified Eagle medium (DMEM), L-glutamine, penicillin and streptomycin, heat-inactivated fetal bovine serum (FBS), Roswell Park Memorial Institute (RPMI) 1640, and 3-(4,5-dimethylthiazol-2-yl)-2,5-diphenyltetrazolium bromide (MTT) were purchased from Sigma (Sigma-Aldrich, St. Louis, US).

2.2 | Peptides

TA, (F¹L²P³L⁴I⁵G⁶R⁷V⁸L⁹S¹⁰G¹¹I¹²L¹³-NH₂), TB (L¹L²P³I⁴V⁵G⁶N⁷L⁸L⁹K¹⁰S¹¹L¹²L¹³-NH₂), and TG (F¹F²P³V⁴I⁵G⁶R⁷I⁸L⁹N¹⁰G¹¹I¹²L¹³-NH₂) peptides were purchased from Biomatik (Wilmington, DE, USA). Each peptide was synthesized by solid-phase Fmoc chemistry methodology. A purity of 95% was obtained via reverse-phase high-performance liquid chromatography (RP-HPLC) using a gradient of 0.1% trifluoroacetic acid in acetonitrile from 20% to 100% in 30 minutes at a flow rate of 1 ml/min (Gemini 5 μm C18 110A HPLC Column 250 × 4.6 mm).²² The molecular mass of the peptides was verified by mass spectrometry. All peptides were dissolved in water; stock solutions of 2 mM were prepared.

2.3 | Cells and viruses production

Human epithelial lung (A549) and Madin-Darby Canine Kidney (MDCK) cells were grown in DMEM and RPMI 1640, respectively, supplemented with 10% FBS, 0.3 mg/mL of L-glutamine, 100 U/mL of penicillin, and 100 μg/mL of streptomycin at 37°C in an atmosphere of 5% CO₂.

Both influenza virus A/Puerto Rico/8/34 H1N1 (PR8 virus) and parainfluenza virus Sendai type 1 (SeV) production was performed by means of 11-day-old embryonated chicken eggs. More precisely, viral suspension was inoculated in the allantoic cavity of embryonated eggs at 37°C for 48 hours; then infected eggs were maintained overnight at 4°C. Subsequently, the allantoic fluid was collected and

centrifuged (2500 g for 30 minutes).²³ The PR8 stock solution titred 1.3×10^{11} plaque-forming unit/mL; the SeV stock solution titred 8.192 hemagglutinating unit (HAU)/mL.

2.4 | Cell toxicity assays

The cytotoxicity of the peptides was evaluated by the inhibition of MTT reduction into formazan crystals^{19,22,24} and by the trypan blue staining assay.²⁵ Particularly, in the MTT assay, A549 cells were seeded in 96-well plates at a density of 2×10^4 cells/well in 100 μL of complete DMEM without phenol red for 24 hours at 37°C. Subsequently, cell monolayers were treated or not with increasing concentrations (0.1, 7.5, 15, 30, 40, 60 μM) of temporins for 24 hours at 37°C. After 24 hours, 10 μL of MTT solution (5 mg/mL) was added to each well for 3-4 hours at 37°C. Each sample was then acidified by adding 0.1 N HCl in isopropanol (100 μL/well) for 30 minutes under mild agitation to ensure the dissolution of all formazan crystals. The absorbance of samples was read at 570 nm, using an automatic plate reader (Multiskan EX, Ascent Software, Thermo Fisher Scientific). Untreated cells were used as control. The 50% cytotoxic concentration (CC₅₀), defined as the peptide concentration required to reduce cell viability by 50%, was calculated by regression analysis of log(dose) response curve generated from the data, using the GraphPad, Prism 6 Software.

2.5 | Viral infection

A549 cells were seeded in 12-well plates at a density of 2.5×10^5 cells/well for 24 hours at 37°C and then infected with PR8 or SeV (multiplicity of infection, MOI = 0.001) for 1 hour at 37°C. After viral adsorption, cell monolayers were washed with phosphate-buffered saline (PBS), supplemented with fresh medium plus 2% FBS, and maintained at 37°C. The viral production was measured in the cell supernatant of infected cells recovered at 24 and 48 hours after infection. The concentration of peptide causing a 50% reduction of viral infection (IC₅₀) was determined by regression analysis using GraphPad Prism v6.0 software by fitting a non-linear log dose-response curve.

2.6 | Viral titration methods

2.6.1 | TCID₅₀ (tissue culture infectious dose 50%) assay

The TCID₅₀ assay is defined as the dilution of a virus required to infect 50% of a cell monolayer. The assay relies on the presence and detection of cytocidal virus particles (ie,

those capable of causing the virus cytopathic effect-CPE). MDCK cells were seeded in 96-well plates at a density of 2×10^4 cells/well for 24 hours at 37°C in an atmosphere of 5% CO₂. Subsequently, cell monolayers were infected for 1 hour at 37°C, using 10-fold dilutions of the samples (8 wells per dilution), previously collected upon infection and/or appropriate peptide treatment. After viral adsorption, cells were washed with PBS, 100 µL of fresh medium supplemented with 2% FBS were added to each well for 24 hours at 37°C and the number of wells showing positive CPE was then scored. TCID₅₀/mL was evaluated by means of the Reed and Muench method.^{26,27}

2.6.2 | Hemagglutinating unit (HAU) assay

As stated above, the viral HA protein binds to sialic acid receptors on cells, including erythrocytes, forming a complete network of linked erythrocytes. The formation depends on the presence of a sufficient amount of virus; when it is low, red blood cells (RBCs) are not constrained by the network and precipitate at the bottom of the plate forming a red button. The hemagglutination property is the basis of a quick assay to estimate the amount of influenza or parainfluenza viruses in a sample.^{26,27} Briefly, twofold serial dilutions of a cell supernatant containing viral particles were added to the wells of 96-well U-bottom microtiter plates and mixed with 0.5% RBCs suspended in PBS, and incubated at room temperature until the formation of red button. The hemagglutinating unit (HAU) corresponds to the virus dilution before red button formation.

To evaluate the ability of TG to directly impair viral agglutination, a solution of the PR8 virus was twofold serially diluted and added to the wells of a microplate and mixed with TG (30 µM). Afterward, RBCs (0.5% in PBS) were added to each well and the plate was incubated at room temperature. If TG interacts with HA, it inhibits the formation of linked erythrocytes which precipitate forming the red button.

2.6.3 | In-cell western (ICW) assay

This is an innovative cell-based technique that allows a rapid, sensitive, and high-throughput quantification of viral proteins expressed on cell monolayers.^{28,29} Briefly, A549 cells were seeded in 96-well plates at a density of 2×10^4 cells/well for 24 hours at 37°C in an atmosphere of 5% CO₂. Confluent cell monolayers were infected with PR8 or SeV for 1 hour at 37°C. After viral adsorption, cells were washed with PBS and then fresh medium supplemented with 2% FBS was added for 24 hours at 37°C. Subsequently, cell monolayers were fixed with 3.7%

formaldehyde for 20 minutes, permeabilized with 0.1% Triton X-100 and incubated with Odyssey blocking buffer (LI-COR Bioscience, Lincoln, NE) for 60 minutes at room temperature. The cells were stained at 4°C overnight with primary antibodies against influenza nucleoprotein (NP) or parainfluenza hemagglutinin-neuraminidase (HN). After incubation, three washes with PBS plus 0.1% Tween 20 were performed and then the cells were stained with a mixture of fluorochrome-conjugated secondary antibodies (fluorescence emission at 800 nm), properly diluted in Odyssey blocking buffer and fluorochrome-conjugated Cell Tag (fluorescence emission at 700 nm), for 1 hour at room temperature. Cell Tag was used as control of the integrity of the cell monolayer. Subsequently, three washes with PBS plus 0.1% Tween 20 were performed and plates were analyzed by the Odyssey infrared imaging system (LI-COR). Integrated intensities of fluorescence were determined by the LI-COR Image Studio software and the relative fluorescence intensity (RFI) was expressed as a percentage compared to untreated infected cells (100%).

2.7 | Western blot analysis

The pellet of cells, collected upon infection and appropriate treatment with the peptide, was suspended in cold lysis buffer (10 mM Tris, 150 mM NaCl, and 0.25% NP-40, pH 7.4) and incubated on ice for 30 minutes. Subsequently, cell lysates were centrifuged (14 500 g, 30 minutes, 4°C); the supernatants were collected and protein concentration was determined by Bradford protein assay. Lysates were diluted in sodium dodecyl sulfate (SDS) sample buffer containing DL-dithiothreitol, separated by SDS-PAGE, and blotted onto nitrocellulose membranes. The membranes were blocked with 10% milk solution (Bio-Rad Laboratories, Berkeley, CA) in T-TBS (0.01% Tween 20 plus Tris-buffered saline) for 1 hour at room temperature and then incubated with a polyclonal goat-anti-influenza antibody overnight at 4°C. Following three washes with T-TBS, the membranes were incubated with a horseradish peroxidase-conjugated secondary antibody. The enhanced chemiluminescence detection system (Thermo Fisher Scientific, Waltham, MA, US) was used to detect blots. Actin was used as a loading control.

2.8 | Time-of-addition assay

A549 cells were seeded in 12-well plates at a density of 2.5×10^5 cells/mL for 24 hours at 37°C, infected with PR8 or SeV (0.001 MOI) and treated or not with TG (30 µM) at different phases of virus life-cycle, as indicated in the Results section. Untreated infected cells were used as control. Cell supernatants and infected monolayers were analyzed to estimate viral

production, virus-induced cytopathic effect, viral protein expression, and synthesis.

2.9 | Attachment assay

A549 cells were seeded in 12-well plates at a density of 2.5×10^5 cells/mL for 24 hours at 37°C and then infected with PR8 and contemporarily treated or not with TG (30 μ M) for 1 hour at +4°C (synchronization phase of the viral infection). Cells were washed with PBS and DMEM was added for 1 hour at 37°C (adsorption phase). Subsequently, cell monolayers were washed again with PBS and fresh complete medium was added for 24 hours at 37°C. Cell supernatants and infected monolayers were analyzed to estimate viral production and viral protein synthesis.

2.10 | Entry assay

A549 cells were seeded in 12-well plates as indicated above, and then infected with PR8 for 1 hour at +4°C to allow virus binding to the cell surface. Subsequently, TG (30 μ M) was added for 1 hour at 37°C. Samples were washed and cell supernatants were analyzed as indicated above.

2.11 | Pre-treatment assay

A549 cells were seeded in 12-well plates as previously described, treated with TG (30 μ M) for 3 hours at 37°C and then infected with PR8 for 1 hour at 37°C. After viral adsorption, cells were washed and their supernatants were analyzed as indicated in the previous paragraph.

2.12 | Hemolysis inhibition assay

The hemolysis inhibition assay was performed as reported earlier³⁰ with minor modification. Briefly, 100 μ L of TG (30 μ M) was mixed with an equal volume of PR8 for 30 minutes at room temperature. Afterward, an equal volume (200 μ L) of 2% RBC was added to the mixture for 30 minutes at 37°C. Subsequently, to trigger hemolysis, 100 μ L of sodium acetate (0.5 M, pH 5.2) was added to the suspension. The mixture was incubated for 30 minutes at 37°C to allow HA acidification and hemolysis. To separate non-lysed erythrocytes, plates were centrifuged at 1200 rpm for 6 minutes at the end of the incubation time. The absorbance of the released hemoglobin in the supernatant was measured at 540 nm using a microtiter plate reader (Multiskan EX, Ascent Software, Thermo Fisher Scientific). Untreated virus and the vehicle PBS were used as positive and negative controls, respectively.

2.13 | Circular dichroism

All CD spectra were recorded using a JASCO J710 spectropolarimeter at 25°C with a cell of 1 mm or 10 mm path length. The CD spectra were acquired by the range from 260 to 190 nm 1 nm bandwidth, 4 accumulations, and 100 nm/min scanning speed. The CD spectra of TA and TG, at a concentration of 50 μ M, were acquired in water (pH = 7.4), in SDS (20 mM) and in dodecylphosphocholine (DPC, 20 mM) micellar solutions.

2.14 | Modeling of the complex of HA with TG

The model of the complex between HA and the peptide TG was obtained by performing docking calculations with the HPEPDOCK software.³¹ The HPEPDOCK is an innovative online server for investigating protein-peptide docking based on the hierarchical algorithm. It performs a blind and flexible peptide docking by fast modeling of peptide conformations and sequent global sampling of binding orientations. Information about available structural data for HA receptor was retrieved and downloaded from the Protein Data Bank (www.pdb.org). These data correspond to the crystal structure of the A/Puerto Rico/8/1934 (H1N1) influenza virus HA (PDB code: 5W6T).³² As input coordinates for peptide, a model obtained by the experimental NMR structure of TA in SDS solution³³ was used in the calculations. In fact, TG has CD spectra very similar to TA³⁴ in different environments (Figure S1). The best three complex structures for the peptide were scored by HPEPDOCK and subjected to refinement using the Refinement Interface of the webserver HADDOCK 2.2³⁵ and scored according to the HADDOCK-scores.³⁵ The Refinement Interface protocol consists of three stages: first, a rigid body energy minimization that generates 20 structures, then a semi-flexible refinement in torsion angle space, and finally refinement in Cartesian space with explicit solvent. The Refinement Interface of HADDOCK 2.2 generates a result (HADDOCK score) based on a weighted sum of Van der Waals, electrostatic, and desolvation energies, buried surface area values in combination with AIRs restraint energy, which has been used as criteria in the selection of the best complex. The best water-refined HADDOCK model was selected for energy (Table S1) and interactions analyses.

2.15 | Statistical analysis

Statistical significance of the data was analyzed by means of a Student t test and *P* values of <.05 were considered significant. Data were expressed as mean \pm the standard deviation (SD).

3 | RESULTS

3.1 | TB and TG are non-cytotoxic on alveolar lung cells

We initially evaluated the cytotoxicity of the three temporin isoforms TA, TB, and TG on A549 cells by performing the MTT assay and by staining them with trypan blue. In both types of assays, cells were treated or not with different concentrations of the peptides and data were analyzed after 24 hours treatment. The MTT assay revealed that TA was more cytotoxic than the other two temporins.

In fact, already at the low concentration of 15 μM , the percentage of metabolically active cells was $74 \pm 15\%$ (Figure 1A), while it significantly dropped at higher doses of TA. In comparison, in the case of TB and TG, the percentage of viable cells resulted to be equal to $64 \pm 16\%$ and $79 \pm 6\%$, respectively, at the higher concentration of 40 μM , ie, 1.6 log(dose). These results were confirmed by the trypan blue staining (data not shown). Moreover, the peptide concentrations causing 50% cytotoxicity (CC_{50}) were determined and found to be equal to 31 μM for TA (95% confidence interval, CI, 26.36-36.23); 58 μM for TB (95% CI, 45.52-92.68) and 73 μM for TG (95% CI, 63.21-95.42).

On the basis of this outcome, TA was excluded from subsequent experiments, while TB and TG were used at a concentration range from 0.1 to 40 μM .

3.2 | Treatment with TG affects influenza virus replication

We initially performed experiments aimed at defining the 50% inhibitory concentration (IC_{50}) of both TB and TG peptides. A549 cells were infected with PR8 and, after viral challenge, different concentrations of the peptides were added to infected cells and maintained for the following 24 hours. Supernatants were then recovered and viral titer was measured by means of HAU assay as described in the Materials and Methods. As reported in Figure 1B, the IC_{50} for TG was found to be 13 μM (95% CI, 9.253 – 17.22) with a Selectivity Index (SI) ($\text{CC}_{50}/\text{IC}_{50}$) of 5.6.

Treatment with TB was less effective giving an IC_{50} of 38 μM (95% CI, 36.49-40.24) with a SI of 1.5 (Figure S2A). Altogether these results indicated that TG was the most effective peptide between the two temporin isoforms. On the basis of these data, the antiviral efficacy of TG was evaluated at different phases of virus life-cycle: (i) during viral adsorption for 1 hour (ADS); (ii) immediately after viral adsorption for 24 hours (POST); (iii) during and after viral adsorption (ADS + POST). We decided to use a peptide concentration of 30 μM , which is ~2.3-fold higher than the corresponding IC_{50} of TG.

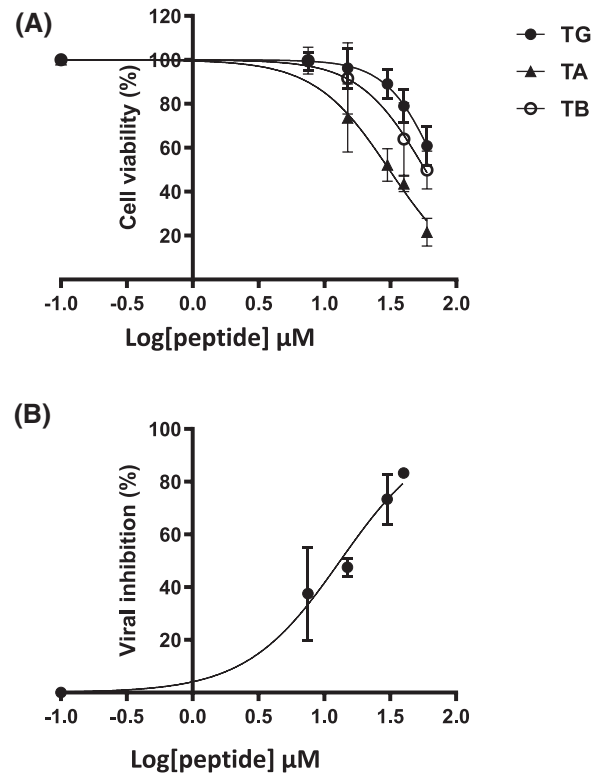


FIGURE 1 TG does not affect the viability of A549 cells compared to TA and TB. A, Cell monolayers were treated or not with increasing concentrations (0.1, 7.5, 15, 30, 40, 60 μM corresponding to -1, 0.87, 1.18, 1.48, 1.6, 1.78 log(dose)) of each peptide for 24 hours and the amount of metabolically active cells was determined by the MTT assay and expressed as a percentage compared to untreated control cells. The CC_{50} of the three peptides was calculated by regression analysis of the dose-response curve. Values are expressed as mean \pm SD from two independent experiments, each performed in duplicate ($n = 4$). B, Influenza virus (PR8)-infected cells were treated with TG at different concentrations (0.1, 7.5, 15, 30, 40 μM), and viral titer inhibition was determined by HAU assay. The IC_{50} of the compound was calculated by regression analysis as described in Materials and Methods

The antiviral efficacy was initially analyzed through the evaluation of the virus-induced CPE (Figure 2A). As expected, infected monolayers (PR8) showed morphological changes, encompassing cell rounding, increased refractility, cell aggregation, and detached cells from the monolayer, while treatment with TG reduced PR8-induced CPE, especially when the peptide was added during ADS and ADS + POST phases. In parallel, supernatants of infected cells were used for the quantification of viral titer (Figure 2B), as described in the Methods Section. The HA protein content in these supernatants was quantified by HAU assay. Although TG treatment was effective at all the phases studied, the most pronounced inhibition was found when the peptide was added during the ADS or ADS + POST phases. To evaluate whether the virus released in the same supernatants was still infective, samples were added to a fresh monolayer and the $\text{TCID}_{50}/\text{mL}$

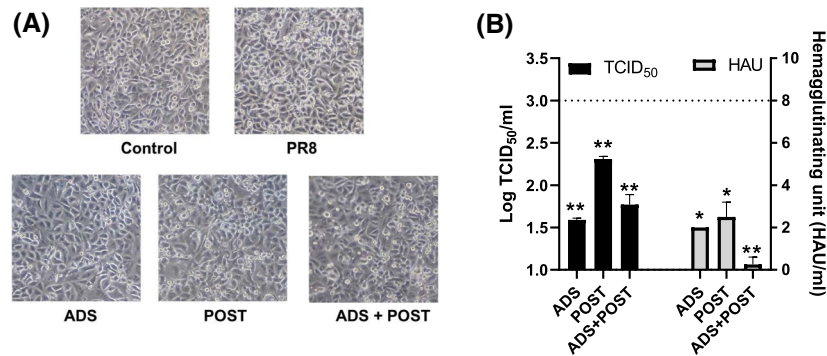


FIGURE 2 TG inhibits PR8 replication at early steps of the virus life-cycle. A549 cells were infected with PR8 and treated or not with the peptide at different phases of the virus life-cycle: (i) during viral adsorption for 1 hour (ADS); (ii) immediately after viral adsorption for 24 hours (POST); (iii) during viral adsorption and for 24 hours (ADS + POST). A, Representative images of the virus-induced cytopathic effect on A549 cells at the different phases of the virus life-cycle upon treatment with TG, compared to uninfected control samples. B, The viral titer in the supernatants of infected cells was analyzed by TCID₅₀ and HAU assay and compared to that of untreated infected cells (dashed line). Values are the mean \pm SD of one representative experiment out of three, each performed in quadruplicate ($n = 4$). Statistical significance of the data vs untreated-infected samples was defined as $*P < .05$ and $**P \leq .01$

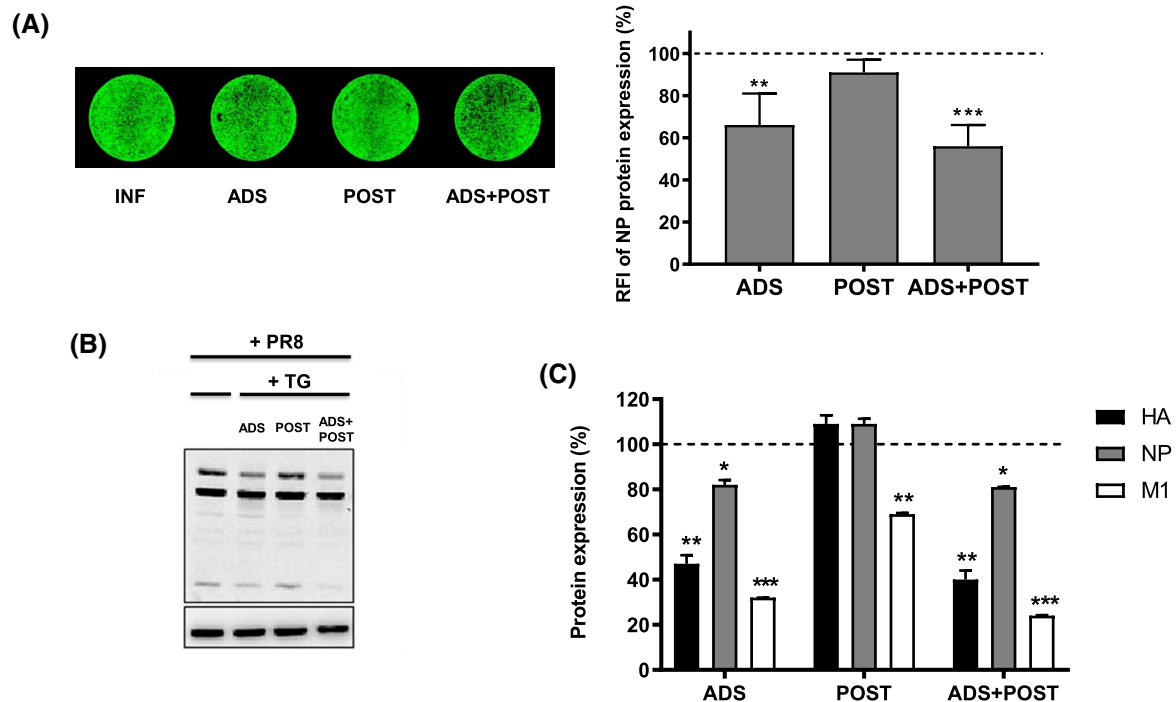


FIGURE 3 TG reduces the expression of viral NP at early phases of the virus-life cycle. A, The expression of NP protein was analyzed on monolayers of A549 cells by ICW assay using LI-COR Image Studio Software to measure the RFI (left side). The graph (right side) represents the percentage of fluorescence intensity calculated in comparison to that of untreated-infected cells (dashed line corresponding to 100%). The values represent the mean \pm SD of four experiments each performed in duplicate ($n = 8$). Statistical significance of data vs untreated-infected cells was defined as $**P < .001$ and $***P < .0001$. B, Cell lysates were also analyzed by western blot to evaluate the expression of the three viral proteins HA, NP, and M1. Actin was used as a loading control. Results are representative of one out of three performed experiments. C, Densitometry analysis of viral proteins. The expression of each protein was normalized to that of actin and expressed as a percentage with respect to that obtained from untreated-infected cells which are indicated by the dashed black line (100%). The results are the mean \pm SD of three independent experiments, ($n = 3$). Statistical significance of data vs untreated-infected cells was defined as $*P < .05$; $**P < .001$ and $***P < .0001$

(dilution of a virus required to infect 50% of a cell monolayer) was calculated. This method confirmed a significant inhibition of viral replication during the ADS or ADS + POST phases compared to untreated infected cells, with 1.41 log or 1.23 log reduction of viral titer (96.1% and 94.1% inhibition,

respectively). Finally, we analyzed the viral protein expression directly on infected cell monolayers, measuring the RFI by ICW assay as described in Methods. As shown in the graph of Figure 3A, a lower expression of viral NP was quantified during ADS and ADS + POST treatment compared to

infected cells (considered as 100%). Furthermore, synthesis of viral proteins (ie, HA, NP, and M1) during the various phases of treatment with TG was analyzed by western blot (Figure 3B). Densitometry analysis highlighted a lowering of the expression level of the three proteins mostly during ADS and ADS + POST phases (Figure 3C), confirming the results obtained from the viral titration assays.

In comparison, when the activity of the isoform TB was evaluated under the same conditions used for TG, only a slight non-significant reduction of viral titer was observed. Indeed, $16 \pm 12\%$ reduction of viral NP expression with respect to untreated infected cells was calculated when TB was added during the infection (ADS) phase (Figure S2B). These findings confirmed a very weak antiviral activity of TB and for this reason, this peptide was not included in the next experiments.

3.3 | Temporin G inhibits the entry of influenza virus into the host cells

Since TG resulted to be more effective during ADS and ADS + POST phases, we explored whether the antiviral activity of this peptide was due to its ability to block some early phases of the PR8 life-cycle. In particular, the attachment and entry of the virus into the host cell was studied through specific assays.²¹ The first assay was performed to assess the ability of TG to interfere with the binding of the virus

to host cell membrane receptors. Particularly, cell monolayers were infected and contemporary treated or not with TG for 1 hour at +4°C (synchronization phase of the viral infection); then, cells were incubated for 1 hour at 37°C to enable viral adsorption. In parallel, the entry assay was carried out to monitor the ability of TG to inhibit the intracellular entry of influenza virus, after its binding to the receptor. In this case, cell monolayers were infected with PR8 for 1 hour at +4°C to allow the attachment of the virus to the cell surface; then, the peptide was added or not for 1 hour at 37°C. The supernatants of infected cells from both types of experiments were analyzed by the HAU assay 24 hours post-infection (p.i.). As reported in Figure 4A, TG strongly affected viral titer during the entry phase, despite it was also effective during the attachment phase. These results are in line with the expression level of viral proteins. Indeed, as highlighted by western blot (Figure 4B) and densitometry analysis (Figure 4C), a decreased protein expression of HA, NP and M1 was detected in both phases, although it was more pronounced during the entry phase. This means that the peptide mainly influences the viral entry into the cells and, as a consequence, it inhibits viral protein synthesis.

Subsequently, we also verified whether TG was able to impair the binding of the virus to the cell. To this aim, cell monolayers were first pre-incubated with TG for 3 hours at 37°C and then infected with the virus. After 24 hours p.i., supernatants were tested by HAU and ICW assays. As illustrated in Figure 5, pre-treatment of cells with the peptide

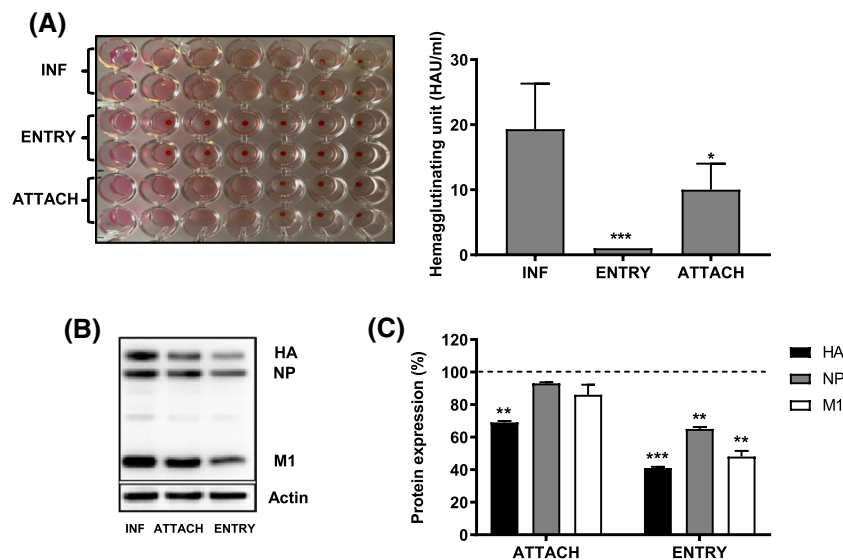


FIGURE 4 TG interferes with the entry phase of the PR8 life-cycle. A, Viral titer in the supernatant of infected cells after peptide treatment was analyzed during the attach and entry phases by HAU assay and compared to that of untreated infected cells (INF). The image shows representative results of one out of three independent experiments (left side). The graph (right side) represents mean values of HAU \pm SD obtained from supernatants of attachment and entry assays compared to INF, of three independent experiments, each performed in duplicate ($n = 6$). B, Cell lysates were analyzed by western blot to evaluate the expression of HA, NP, and M1 viral proteins. Actin was used as a loading control. C, Densitometry analysis of viral proteins. Expression of each protein was normalized to that of actin and expressed as a percentage with respect to the amount obtained from untreated-infected cells, which is indicated by the dashed line (100%). The results are the mean \pm SD of three independent experiments ($n = 3$). Statistical significance of data vs untreated-infected cells was defined as * $P < .05$; ** $P < .001$ and *** $P < .0001$

before the addition of the virus did not provoke any change in the virus titer or the expression of NP protein compared to untreated infected cells. This endorses the notion that TG does not compete with the binding of influenza virus to host cell receptors.

3.4 | The antiviral activity of TG is related to the peptide ability to prevent the conformational change in the viral HA2 subunit

The viral HA plays a critical role in virus entry; the mature HA protein is composed of two disulfide-linked subunits, HA1 and HA2. The first one is responsible for virus binding, while the HA2 subunit mediates virus-cell fusion. Thus, to get insight into the mechanism by which TG impairs viral entry into host cells, we first evaluated whether TG directly interacted with HA protein by performing a hemagglutination inhibition assay, slightly modified as described in Methods. To this aim, a solution of PR8 (the same concentration used for the infection of cells) was twofold serially diluted and pre-incubated with or without the peptide for 1 hour at 37°C. Afterward, 0.5% of RBCs were added and incubated at room temperature to allow the formation of red button. The results of the experiments indicated that in the presence of TG, virus-RBCs agglutination was markedly reduced compared to what found for the virus solution not-treated with the peptide (Figure 6A).

The second aim was to study whether TG interfered with the viral-cell membrane fusion. Notably, once viral particles are internalized into endosomes, the low pH inside the

endosomal vesicle activates viral M2 protein that functions as a proton channel. The acidification inside viral particles causes a conformational change in the HA2 subunit leading to the exposure of its N-terminal fusion peptide and hence favoring the fusion between the viral envelope and the endosomal membrane.³⁶ We carried out a hemolysis inhibition assay, as described in Methods.³⁰ Briefly, a solution of 2% of RBCs was mixed with an equal volume of TG and PR8, and the lysis of erythrocytes, obtained by the acidification of virus-cell suspension, was evaluated by measuring the amount of released hemoglobin. As shown in Figure 6B, TG reduced by 77% the release of hemoglobin compared to what was obtained in the presence of the virus alone. These results denoted the occurrence of interaction between TG and HA; this would prevent the conformational change in HA thus limiting the availability of HA2 subunit in the active form and therefore the virus-cell fusion.

3.5 | TG binds HA stem groove at the HA1/HA2 interface

To support the ability of TG to impede the virus-endosomal cell membrane fusion by direct interaction of the peptide with HA, molecular docking studies were performed. HA crystal structure³² was docked with a model structure of TG obtained starting from the solution structure of TA.³³ In fact, TG and TA share very similar CD spectra in water and membrane mimetic environments (Figure S1). Docking was performed with the HPEPDOCK³¹ program and the best scored pose was optimized by the Refinement Interface of the HADDOCK program suite.³⁵ Complex energy terms are indicated in Table S1. TG/HA complex model obtained by docking procedure is reported in Figure 7. TG showed a helix structure encompassing residues 4-10 with N- and C-terminal segments in a more extended conformation. TG recognized the highly conserved hydrophobic membrane-proximal stem groove formed by HA2 and the N- and C-terminal regions of HA1 (Figure 7A). Numerous nonpolar contacts were made by the hydrophobic residues in the peptide (Figure 7B). Accordingly, Van der Waals energy term was the most important in the complex stabilization (Table S1). In particular, Phe² of TG lied in a hydrophobic pocket formed by Gly²⁰, Trp²¹, Thr⁴¹, and Ile⁴⁵ of HA2. It made edge-to-face aromatic interactions with Trp²¹. Interestingly, edge-to-face aromatic interaction between a conserved Phe (from different locations) and HA2 Trp²¹ was observed in the complexes of other peptides and antibodies able to bind to group 1 H1 HA.^{32,37,38} Furthermore, Trp²¹, together with Tyr²² and Gly²³, represent the highly conserved C-terminal region of the fusion peptide (HAfp23).³⁹

Overall, these results have demonstrated that TG likely binds HA at the HA1/HA2 interface, suggesting its

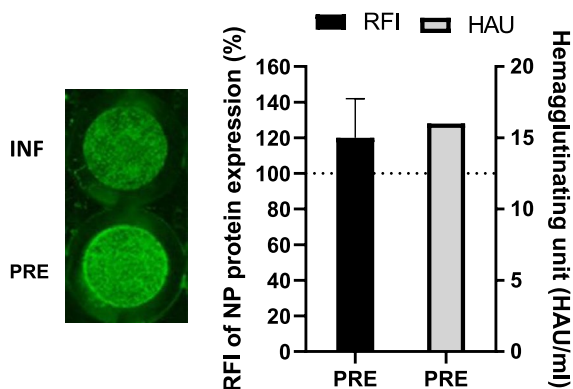


FIGURE 5 Pre-treatment of A549 cells with TG does not affect the replication of PR8. A549 cell monolayers were pre-treated (PRE) or not (INF) with TG for 3 hours at 37°C and then infected with PR8 for 1 hour at 37°C. At 24 hours p.i. supernatants were collected for HAU assay, while cell monolayers were analyzed for NP expression by ICW assay (left side). The results of viral titers and NP protein expression are expressed as HAU and as a percentage of protein expression compared to untreated-infected cells (dashed line), respectively, and are the mean \pm SD of two independent experiments, each performed in duplicate, ($n = 4$) (right side)

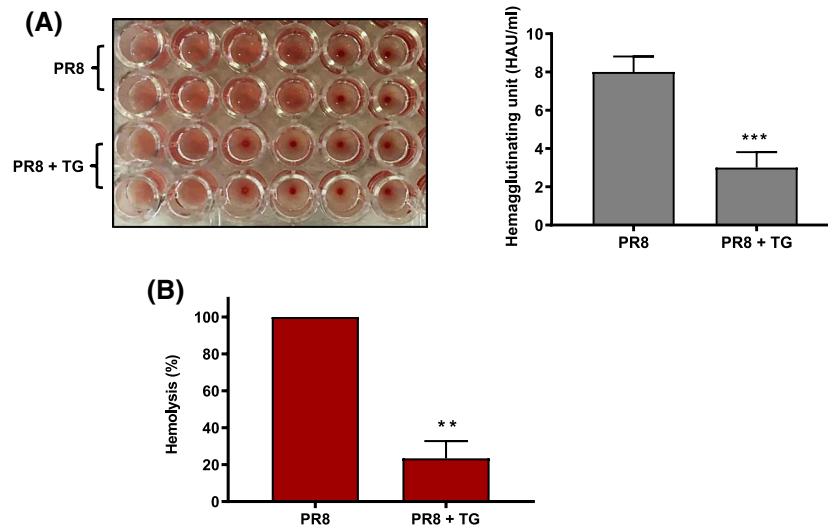


FIGURE 6 TG inhibits viral agglutination and lysis of RBC. A, PR8 solution was twofold serially diluted and pre-incubated or not with the peptide (30 μ M) and then analyzed for its ability to agglutinate RBCs (left side). The graph (right side) represents the mean values \pm SD of HAU obtained from two independent experiments, each performed in duplicate, ($n = 4$). B, PR8 and TG were mixed for 30 minutes at room temperature; afterward, an equal volume of 2% RBC was added to the mixture for other 30 minutes at 37°C. Subsequently, sodium acetate was added for 30 minutes at 37°C, to lower the pH and trigger hemolysis. The absorbance of the released hemoglobin was measured from the samples' supernatant. Results are expressed as the percentage of hemolysis compared to that provoked by untreated PR8. Values are the mean \pm SD from two independent experiments, each performed in duplicate, ($n = 4$). Statistical significance of data vs PR8 was defined as ** $P < .001$ and *** $P < .0001$

interference with the membrane fusion process during influenza virus entry into the cell.

3.6 | Temporin G inhibits Sendai virus replication

To expand our knowledge on the activity of TG against other respiratory viruses, we examined the antiviral efficacy of this peptide against SeV, a parainfluenza virus type 1 that shares similar characteristics with influenza virus, such as the presence of an HN protein with a dual function. Indeed, HN works as hemagglutinin (which binds to sialic acid) as well as neuraminidase (a sialidase that favors the viral spread). Differently from influenza viruses, SeV enters into cells by direct fusion of the viral envelope with the cell membrane.⁴⁰

A549 cells were infected with SeV and treated or not with TG at different phases of the virus life-cycle, following the same procedure described for PR8. Surprisingly, in contrast with what was obtained for the influenza virus model of infection, the results showed significant activity of TG in two phases of treatment: POST and ADS + POST (Figure 8A). Indeed, viral titer, measured by TCID₅₀ assay, was reduced to ~ 1.2 log in both phases of treatment (Figure 8A). Similarly, the HAU assay showed the highest inhibition of viral replication during POST and ADS + POST phases (~ 3.5 -fold reduction of viral titer with respect to untreated infected cells). In comparison, only a slight reduction of viral titer was found when TG was added during viral adsorption (ADS). Finally,

the expression of the viral HN protein after TG treatment was analyzed by ICW assay (Figure 8B). Unlike what was observed for virus titers in the supernatants of infected cells (Figure 8A), a slight decrease of HN protein expression was found only during the ADS and ADS + POST phases, while no differences were observed when TG was added after viral adsorption (POST). These apparent contrasting data suggested that TG blocked some late steps of viral replication, thus maintaining viral particles into the cells and hence impairing their release into the supernatant.

4 | DISCUSSION

The threat of influenza pandemic all over the world has dramatically augmented during the past decades in parallel with a huge spread of several influenza virus strains.⁴¹ The raising resistance to traditional antivirals has encouraged research to identify new strategies for antiviral therapy.⁴² In this context, AMPs represent attractive novel compounds.⁴³ In the current study, we initially investigated the activity of three isoforms of temporins AMP family, ie, TA, TB, and TG against influenza A PR8 virus. Our data proposed TG as the most effective antiviral peptide without inherent cytotoxicity. As shown by the viral titration assay and the expression of viral proteins, TG was able to affect the early stages of the influenza virus replication cycle by promoting a significant reduction in the viral titer when peptide treatment occurred during the adsorption phase of PR8 to A549

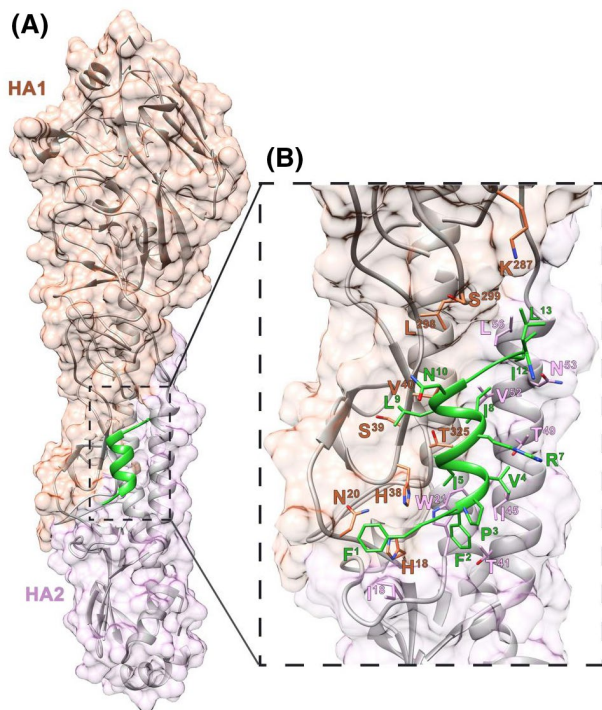


FIGURE 7 TG recognizes the stem groove at the HA1/HA2 interface. A, Model complex of HA and TG: HA is shown in ribbon and surface representation (HA1, light orange; HA2, light pink), while TG is shown as green ribbon. B, TG within the stem groove of HA. Side chain of interacting residues is shown as sticks with carbon atoms in green (TG), light orange (HA1), and light pink (HA2). Residue labels follow the same color code. Nitrogen and oxygen atoms are in blue and red, respectively. Hydrogen atoms are not shown for clarity

cells. Furthermore, this effect had a larger extent when peptide treatment lasted during and after cell infection. The *in vitro* test based on the hemagglutinating capacity of HA protein confirmed the existence of peptide interaction with the viral particle, and precisely with HA. This led to the hypothesis that TG can bind either to the receptor-binding site on the HA1 subunit, preventing the virus from attaching to the host cell, or to the membrane-proximal stem formed by the HA2 subunit and the N- and C-terminal regions of HA1, preventing the conformational change in this viral protein, which is essential for the endocytosis of the virus inside the host cell. However, virological tests (attachment and entry assay) clearly suggested that TG mainly hampers the virus entry rather than the attachment phase. This was also supported by the hemolysis inhibition assay at low pH, which pointed out a consistent lower percentage of hemoglobin released from RBCs when the virus was incubated with the peptide, compared to the results found in the absence of TG. Remarkably, this finding suggests the ability of this peptide to block the large conformational rearrangements of the HA2 subunit, which are associated with membrane fusion, thereby neutralizing the virus. These data are also sustained by molecular docking studies showing TG/

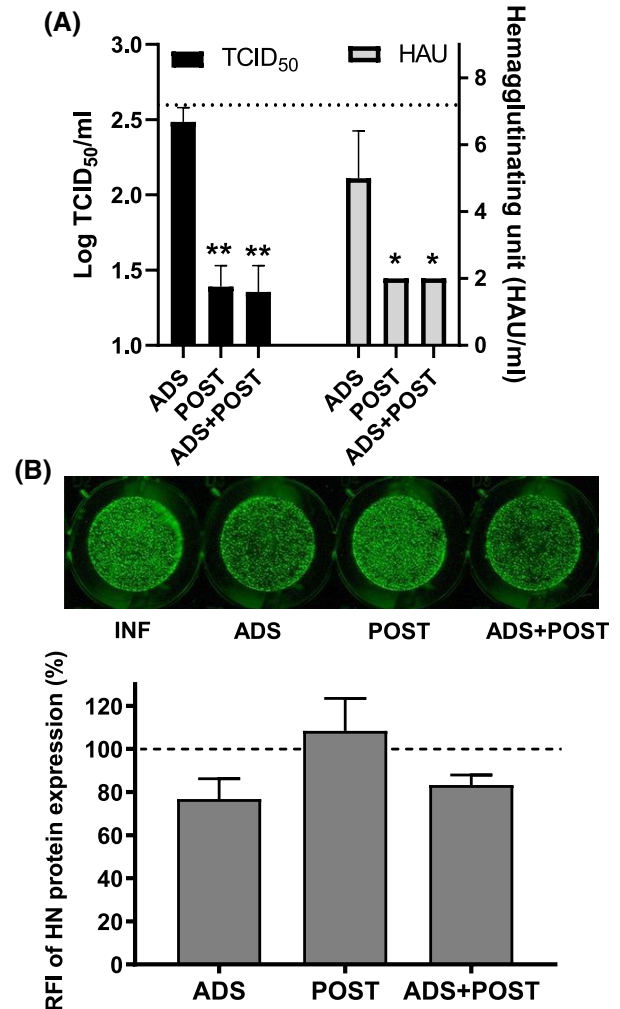


FIGURE 8 TG inhibits the replication of SeV. A549 cells were infected with SeV and treated or not with TG at different phases of the parainfluenza virus life-cycle, as described for PR8. A, The supernatants of infected cells were analyzed by TCID₅₀ and HAU assays. Dashed black line indicates the viral titer of untreated-infected cells. The results are the mean \pm SD from two independent experiments, each performed in duplicate, ($n = 4$). Statistical significance of data vs untreated-infected cells was defined as * $P < .05$ and ** $P < .01$. B, The expression of the viral HN protein, in various phases of treatment with TG, was analyzed by ICW assay, using LI-COR Image Studio Software to measure the RFI. The percentage of fluorescence intensity was calculated in comparison to that of untreated-infected cells (dashed line which corresponds to 100%). The results are the mean \pm SD from two independent experiments, each performed in duplicate, ($n = 4$)

HA complex formation through the TG recognition of the highly conserved hydrophobic stem groove of HA.

Note that we first showed the ability of a peptide belonging to the temporins family, and in general to AMPs, to hinder the early phases of influenza virus replication, likely due to its interaction with HA stem groove to prevent the endocytosis process for the viral entry into the cell.

Furthermore, with the aim to explore the activity of temporins on other respiratory viruses, the isoform TG was also analyzed against SeV. This latter replicates by a different mechanism, especially with reference to the entry phase. In fact, this virus uses the surface protein HN to attach to the host cell and the F protein to be taken by the cell, upon fusion.⁴⁴ The results obtained from the analysis of cell supernatants underscored a consistent lowering in the titer of new virions released from the infected cells. The detection of HN protein by ICW on the cell monolayer revealed, a decreased expression of this protein, although not significant, when peptide treatment occurred during the ADS phase and, consequently, during ADS + POST treatment, while an increased expression level of HN was manifested during the POST phase treatment. The apparent controversial results obtained by the two methods (one measuring viral particles released from infected cells; the other one quantifying the expression of viral proteins inside the cells), indicate that TG retains virions into infected cells, probably by interfering with sialidase activity of HN. As a result, the number of viral proteins in the cells is augmented, while the virus release is hampered. The fact that SeV uses F protein to fuse its envelope with the cell membrane led to the hypothesis that TG also hinders cell-to-cell spread. Further studies are in progress to validate this assumption.

Overall, the achievements of the present study have clearly demonstrated that TG has antiviral activity on both influenza and parainfluenza viruses with a distinct mechanism that relies on (i) the inhibition of virus entry into the host cells, for PR8, and on (ii) the inhibition of the budding phase in the case of Sendai. Taking into account the different ways of cell entry by the two viruses, it can be speculated that the peptide acts intracellularly by blocking the conformational change in the flu virus HA which is necessary for allowing the fusion of viral and endosomal membranes with subsequent dissemination of the viral genome. Otherwise, in the case of parainfluenza virus, since its entry phase is mediated by the fusion protein, the virus would enter the cell, would complete its replication and transcription processes, while the release of the new virions would be impeded by the interaction of TG with HN, inside the cell. Remarkably, since other respiratory viruses, eg, severe acute respiratory syndrome coronavirus (SARS-CoV) use the viral *spike* protein to activate the fusion process after attachment to the cell receptor,⁴⁵ it is expected that temporins are active also against these viruses.

In line with other membrane-active temporins, it is not surprising that TG can penetrate into mammalian cells to explicate its antiviral power.¹⁹ Regarding the uncommon target of TG compared to that of available anti-flu drugs, this peptide may also have a synergistic effect when combined with current antiviral agents. The usage of multiple molecules can warrant a more efficient treatment of viral respiratory infections. In fact, this would decrease the dosage of each

compound and therefore the potential side effects, limiting the appearance of drug-resistant viruses that can conduct to an inevitable therapeutic failure.

Importantly, for the treatment of influenza virus infections, pulmonary delivery of drugs is the simplest administration route to address infected cells. Despite AMPs have a high susceptibility to proteolytic degradation, advances in nanotechnologies have made it possible to overcome this drawback by conjugating AMPs with nanocarriers, such as nanoparticles (NPs) or liposomes.^{46,47} In support of this, recent studies have emphasized that polyvinyl alcohol-engineered poly(lactic-co-glycolic) acid NPs are a reliable nanocarrier to assist the delivery of AMPs in the conductive airways. When AMP-loaded NPs were administered intratracheally in mice with bacterial lung infection, they turned out to be an enticing nanoformulation to prolong the therapeutic efficacy of the encapsulated peptide, in comparison to the corresponding AMP in the free soluble form.⁴⁸

Peptides able to obstruct the entry of virus particles have already been identified as encouraging candidates for viral therapy application. As an example, FluPep, which is a mix of hydrophobic α -helical peptides, is capable of interacting with HA to inhibit viral fusion^{49,50}; Flufirvitide can block the binding of HA to sialic acid.^{51,52} Considering that viral infection in the lungs is often followed by bacterial infection, the employment of AMPs targeting both viruses and bacterial species, as for temporins, would be highly advantageous for efficient eradication of respiratory infections. The human AMP cathelicidins do possess antiviral activity against influenza virus upon a direct interaction with the viral envelope followed by its destabilization, without affecting viral aggregation or virus uptake by the cells.⁵³ Salvatore and coworkers have discovered that the human β -defensin 1 interferes with the replication of influenza virus by modulating protein kinase C activity in infected cells.⁵⁴ Previous studies with another amphibian skin AMP, urumin, reported a virucidal activity against influenza virus A (H1N1), likely due to the ability of the peptide to disrupt virus integrity. It was proposed that this happens upon the binding of the peptide to HA1 protein but no experimental evidence on the mechanism by which urumin lysis the virus was provided, neither computational studies aimed at addressing putative binding sites of the peptide to HA were performed.⁵⁵

Overall, our results have disclosed for the first time the ability of an AMP to interfere with influenza and parainfluenza virus replication with a different mechanism. This will open a new avenue for novel therapeutic approaches based on inhalable peptide formulations to fight a large variety of viral respiratory infections, regardless of the virus cell entry mechanism, likely including those caused by the recent pandemic coronavirus SARS-CoV2, which uses both endocytosis and fusion cell processes⁵⁶ and for which the search for specific drugs is still ongoing.⁵⁷

ACKNOWLEDGMENTS

This work was partially supported by the Italian Ministry of Instruction, Universities and Research—MIUR PRIN 2017 2017BMK8JR006 (project “ORIGINALE CHEMIAE in Antiviral Strategy—Origin and Modernization of Multi-Component Chemistry as a Source of Innovative Broad Spectrum Antiviral Strategy”) (LN), MIUR PONARS 01_00597_OR4 (ATP) grants, Fondazione Cenci Bolognetti Istituto Pasteur Italia (LN) grants and Ateneo grants (LN), a grant from Pasteur-Italia Fondazione Cenci Bolognetti “Anna Tramontano 2018” (MLM) and a grant from Sapienza University “RM11816436113D8A” (MLM).

CONFLICT OF INTEREST

The authors have stated explicitly that there are no conflicts of interest in connection with this article.

AUTHOR CONTRIBUTIONS

M. De Angelis, B. Casciaro, A. Genovese, D. Brancaccio, ME Marcocci, A. Carotenuto performed research and analyzed data; E. Novellino and A. T. Palamara reviewed the manuscript. L. Nencioni and M. L. Mangoni designed and supervised research, analyzed data, wrote and edited the manuscript, equally contributing to the work. All authors read and approved the final manuscript.

ORCID

M. L. Mangoni  <https://orcid.org/0000-0002-5991-5868>

L. Nencioni  <https://orcid.org/0000-0003-4427-4823>

REFERENCES

1. WHO. Influenza (seasonal). [https://www.who.int/news-room/fact-sheets/detail/influenza-\(seasonal\)](https://www.who.int/news-room/fact-sheets/detail/influenza-(seasonal))
2. Taubenberger JK, Morens DM. The pathology of influenza virus infections. *Annu Rev Pathol.* 2008;3:499-522.
3. Bouvier NM, Palese P. The biology of influenza viruses. *Vaccine.* 2008;26(Suppl 4):D49-53.
4. Episcopio D, Aminov S, Benjamin S, et al. Atorvastatin restricts the ability of influenza virus to generate lipid droplets and severely suppresses the replication of the virus. *Faseb J.* 2019;33:9516-9525.
5. Nayak DP, Balogun RA, Yamada H, Zhou ZH, Barman S. Influenza virus morphogenesis and budding. *Virus Res.* 2009;143:147-161.
6. Schroeder C, Heider H, Moncke-Buchner E, Lin TI. The influenza virus ion channel and maturation cofactor M2 is a cholesterol-binding protein. *Eur Biophys J.* 2005;34:52-66.
7. Nayak DP, Hui EK, Barman S. Assembly and budding of influenza virus. *Virus Res.* 2004;106:147-165.
8. Samji T. Influenza A: understanding the viral life cycle. *Yale J Biol Med.* 2009;82:153-159.
9. Osterholm MT, Kelley NS, Sommer A, Belongia EA. Efficacy and effectiveness of influenza vaccines: a systematic review and meta-analysis. *Lancet Infect Dis.* 2012;12:36-44.
10. Mifsud EJ, Hayden FG, Hurt AC. Antivirals targeting the polymerase complex of influenza viruses. *Antiviral Res.* 2019;169:104545.
11. Davidson S. Treating Influenza Infection, From Now and Into the Future. *Front Immunol.* 2018;9:1946.
12. Mookherjee N, Anderson MA, Haagsman HP, Davidson DJ. Antimicrobial host defence peptides: functions and clinical potential. *Nat Rev Drug Discov.* 2020;19:311-332.
13. Lakshmaiah Narayana J, Mishra B, Lushnikova T, et al. Two distinct amphipathic peptide antibiotics with systemic efficacy. *Proc Natl Acad Sci U S A.* 2020.
14. Yu Y, Cooper CL, Wang G, et al. Engineered human cathelicidin antimicrobial peptides inhibit Ebola virus infection. *Science.* 2020;23.
15. Mangoni ML. Temporins, anti-infective peptides with expanding properties. *Cell Mol Life Sci.* 2006;63:1060-1069.
16. Grieco P, Carotenuto A, Auriemma L, et al. The effect of d-amino acid substitution on the selectivity of temporin L towards target cells: identification of a potent anti-Candida peptide. *Biochim Biophys Acta.* 2013;1828:652-660.
17. Mangoni ML, Grazia AD, Cappiello F, Casciaro B, Luca V. Naturally occurring peptides from Rana temporaria: Antimicrobial properties and more. *Curr Top Med Chem.* 2016;16:54-64.
18. Mangoni ML, Carotenuto A, Auriemma L, et al. Structure-activity relationship, conformational and biological studies of temporin L analogues. *J Med Chem.* 2011;54:1298-1307.
19. Di Grazia A, Luca V, Segev-Zarko LA, Shai Y, Mangoni ML. Temporins A and B stimulate migration of HaCaT keratinocytes and kill intracellular *Staphylococcus aureus*. *Antimicrob Agents Chemother.* 2014;58:2520-2527.
20. Mangoni ML, Saugar JM, Dellisanti M, Barra D, Simmaco M, Rivas L. Temporins, small antimicrobial peptides with leishmanicidal activity. *J Biol Chem.* 2005;280:984-990.
21. Marcocci ME, Amatore D, Villa S, et al. The amphibian antimicrobial peptide temporin B inhibits in vitro herpes simplex virus 1 infection. *Antimicrob Agents Chemother.* 2018;62.
22. Casciaro B, Loffredo MR, Cappiello F, Verrusio W, Corleto VD, Mangoni ML. Frog skin-derived peptides against *Corynebacterium jeikeium*: Correlation between antibacterial and cytotoxic activities. *Antibiotics (Basel).* 2020;9.
23. Matarrese P, Nencioni L, Checconi P, et al. Pepstatin A alters host cell autophagic machinery and leads to the decrease of influenza A virus production. *J Cell Physiol.* 2011;226:3368-3377.
24. Mosmann T. Rapid colorimetric assay for cellular growth and survival: application to proliferation and cytotoxicity assays. *J Immunol Methods.* 1983;65:55-63.
25. Strober W. Trypan blue exclusion test of cell viability. *Curr Protoc Immunol.* 2015;111(1). <https://doi.org/10.1002/0471142735.ima03bs111>
26. Di Sotto A, Checconi P, Celestino I, et al. Antiviral and antioxidant activity of a hydroalcoholic extract from *Humulus lupulus L.* *Oxid Med Cell Longev.* 2018;2018:5919237.
27. Hierholzer JC, Killington RA. Virus isolation and quantitation. In: Kangro H, Mahy B. *Virology methods manual.* Academic press; 1996; cap. 2: 35–46.
28. Wan Y, Zhou Z, Yang Y, Wang J, Hung T. Application of an In-Cell Western assay for measurement of influenza A virus replication. *J Virol Methods.* 2010;169:359-364.
29. Bizzarri BM, Fanelli A, Piccinino D, et al. Synthesis of stilbene and chalcone inhibitors of influenza A virus by SBA-15 supported Hoveyda-Grubbs metathesis. *Catalysts.* 2019;9:983.

30. Basu A, Antanasijevic A, Wang M, et al. New small molecule entry inhibitors targeting hemagglutinin-mediated influenza A virus fusion. *J Virol.* 2014;1447-1460.
31. Zhou P, Jin B, Li H, Huang SY. HPEPDOCK: a web server for blind peptide-protein docking based on a hierarchical algorithm. *Nucleic Acids Res.* 2018;46:W443-W450.
32. Kadam RU, Juraszek J, Brandenburg B, et al. Potent peptidic fusion inhibitors of influenza virus. *Science.* 2017;358:496-502.
33. Carotenuto A, Malfi S, Saviello MR, et al. A different molecular mechanism underlying antimicrobial and hemolytic actions of temporins A and L. *J Med Chem.* 2008;51:2354-2362.
34. Grieco P, Luca V, Auriemma L, et al. Alanine scanning analysis and structure-function relationships of the frog-skin antimicrobial peptide temporin-1Ta. *J Pept Sci.* 2011;17:358-365.
35. van Zundert G, Rodrigues J, Trellet M, et al. The HADDOCK2.2 Web Server: user-friendly integrative modeling of biomolecular complexes. *J Mol Biol.* 2016;428:720-725.
36. van de Wakker SI, Fischer MJE, Oosting RS. New drug-strategies to tackle viral-host interactions for the treatment of influenza virus infections. *Eur J Pharmacol.* 2017;809:178-190.
37. Corti D, Voss J, Gamblin SJ, et al. A neutralizing antibody selected from plasma cells that binds to group 1 and group 2 influenza A hemagglutinins. *Science.* 2011;333:850-856.
38. Dreyfus C, Laursen NS, Kwaks T, et al. Highly conserved protective epitopes on influenza B viruses. *Science.* 2012;337:1343-1348.
39. Zhang Y, Xu C, Zhang H, Liu GD, Xue C, Cao Y. Targeting Hemagglutinin: approaches for broad protection against the influenza A virus. *Viruses.* 2019;11(5):405. <https://doi.org/10.3390/v11050405>
40. Branche AR, Falsey AR. Parainfluenza virus infection. *Semin Respir Crit Care Med.* 2016;37:538-554.
41. Berkhout B, Sanders RW. Molecular strategies to design an escape-proof antiviral therapy. *Antiviral Res.* 2011;92:7-14.
42. Krol E, Rychlowska M, Szewczyk B. Antivirals—current trends in fighting influenza. *Acta Biochim Pol.* 2014;61:495-504.
43. Sierra JM, Fuste E, Rabanal F, Vinuesa T, Vinas M. An overview of antimicrobial peptides and the latest advances in their development. *Expert Opin Biol Ther.* 2017;17:663-676.
44. Saladino R, Ciambecchini U, Nencioni L, Palamara AT. Recent advances in the chemistry of parainfluenza-I (Sendai) virus inhibitors. *Med Res Rev.* 2003;23:427-455.
45. Du L, He Y, Zhou Y, Liu S, Zheng BJ, Jiang S. The spike protein of SARS-CoV—a target for vaccine and therapeutic development. *Nat Rev Microbiol.* 2009;7:226-236.
46. Casciaro B, Cappiello F, Loffredo MR, Ghirga F, Mangoni ML. The potential of frog skin peptides for anti-infective therapies: the case of esculentin-1a(1–21)NH₂. *Curr Med Chem.* 2020;27:1405-1419.
47. Casciaro B, Ghirga F, Quaglio D, Mangoni ML. Inorganic gold and polymeric poly(Lactide-co-glycolide) nanoparticles as novel strategies to ameliorate the biological properties of antimicrobial peptides. *Curr Protein Pept Sci.* 2020;21:429-438.
48. Casciaro B, d'Angelo I, Zhang X, et al. Poly(lactide-co-glycolide) nanoparticles for prolonged therapeutic efficacy of esculentin-1a-derived antimicrobial peptides against *Pseudomonas aeruginosa* lung infection: in vitro and in vivo studies. *Biomacromol.* 2019;20:1876-1888.
49. Ahmed CM, Dabelic R, Waiboci LW, Jager LD, Heron LL, Johnson HM. SOCS-1 mimetics protect mice against lethal poxvirus infection: identification of a novel endogenous antiviral system. *J Virol.* 2009;83:1402-1415.
50. Nicol MQ, Ligertwood Y, Bacon MN, Dutia BM, Nash AA. A novel family of peptides with potent activity against influenza A viruses. *J Gen Virol.* 2012;93:980-986.
51. Cederlund A, Gudmundsson GH, Agerberth B. Antimicrobial peptides important in innate immunity. *FEBS J.* 2011;278:3942-3951.
52. Skalickova S, Heger Z, Krejcová L, et al. Perspective of use of antiviral peptides against influenza virus. *Viruses.* 2015;7:5428-5442.
53. Tripathi S, Teclé T, Verma A, Crouch E, White M, Hartshorn KL. The human cathelicidin LL-37 inhibits influenza A viruses through a mechanism distinct from that of surfactant protein D or defensins. *J Gen Virol.* 2013;94:40-49.
54. Salvatore M, Garcia-Sastre A, Ruchala P, Lehrer RI, Chang T, Klotman ME. Alpha-Defensin inhibits influenza virus replication by cell-mediated mechanism(s). *J Infect Dis.* 2007;196:835-843.
55. Holthausen DJ, Lee SH, Kumar VTV, et al. An amphibian host defense peptide is virucidal for human H1 hemagglutinin-bearing influenza viruses. *Immunity.* 2017;46:587-595.
56. Shang J, Wan Y, Luo C, et al. Cell entry mechanisms of SARS-CoV-2. *Proc Natl Acad Sci USA.* 2020;117:11727-11734.
57. Checconi P, De Angelis M, Marocchi ME, et al. Redox-modulating agents in the treatment of viral infections. *Int J Mol Sci.* 2020;21(11):4084. <https://doi.org/10.3390/ijms21114084>

SUPPORTING INFORMATION

Additional Supporting Information may be found online in the Supporting Information section.

How to cite this article: De Angelis M, Casciaro B, Genovese A, et al. Temporin G, an amphibian antimicrobial peptide against influenza and parainfluenza respiratory viruses: Insights into biological activity and mechanism of action. *The FASEB Journal.* 2021;35:e21358. <https://doi.org/10.1096/fj.202001885RR>